Nuclear Instruments and Methods in Physics Research B 268 (2010) 1676–1681

Contents lists available at ScienceDirect

Nuclear Instruments and Methods in Physics Research B

journal homepage: www.elsevier.com/locate/nimb

Artificial neural networks for instantaneous analysis of real-time Rutherford backscattering spectra

J. Demeulemeester [a,*], D. Smeets [a,1], N.P. Barradas [b,c], A. Vieira [d], C.M. Comrie [e], K. Temst [a], A. Vantomme [a]

[a] Instituut voor Kern- en Stralingsfysica and INPAC, K.U. Leuven, Celestijnenlaan 200D, B-3001 Leuven, Belgium
[b] Instituto Tecnológico e Nuclear, Estrada Nacional 10, Apartado 21, 2686-953 Sacavém, Portugal
[c] Centro de Física Nuclear da Universidade de Lisboa, Av. Prof. Gama Pinto 2, 1699 Lisboa Codex, Portugal
[d] Instituto Superior de Engenharia do Porto, Rua S. Tome, 4200 Porto, Portugal
[e] Department of Physics, University of Cape Town, Rondebosch 7700, South Africa

ARTICLE INFO

Article history:
Received 21 December 2009
Received in revised form 16 February 2010
Available online 6 March 2010

Keywords:
Artificial neural networks
Real-time RBS
Ni silicides
Growth kinetics
IBA software
RBS analysis

ABSTRACT

This paper reports on the advantage of using artificial neural networks (ANNs) to analyze large sets of real-time Rutherford backscattering spectrometry (RBS) data. Real-time RBS, i.e. collecting RBS spectra at periodic time intervals during a thermal treatment, probes the full response of a thin film to the annealing *in situ*. Although very valuable insights can be gained by this technique, the time-consuming analysis of the vast amount of RBS spectra acquired during real-time RBS measurements has so far prevented the widespread use of real-time RBS. Setting up an ANN is quite an intensive process as well, but once trained, these ANNs can handle the analysis of large data sets practically instantaneously. As such, the beneficial combination of real-time RBS and ANN analysis forms a perfect synergy. In this test case, a network was trained and applied to analyze the Ni silicide growth during annealing of a thin 80 nm Ni film on Si(100). The ANN performance was validated by comparing the ANN results with the conventional analysis performed on the same data set.

1. Introduction

Over the last decades, Rutherford backscattering spectrometry (RBS) has secured an indispensable position as a tool for dedicated compositional depth profile studies in a wide variety of research fields. The main reason for the success of this ion beam technique is that it is fully quantitative and depth-sensitive in a range of a few nm up to tens of μm. In thin film studies RBS is often applied in the cook-and-look approach, in which several specimens are subjected to a thermal treatment and subsequently analyzed by RBS. With this method various features of the solid phase reaction such as thin film phase formation, diffusion kinetics, impurity redistribution, dominant diffusing species, etc. can be studied by examining a number of discrete steps in the thermal treatment. Although this cook-and-look approach has proven very useful in the past, performing RBS *in situ* during the thermal treatment, i.e. *real-time* RBS, yields more valuable and reliable data [1,2]. Moreover, since RBS provides direct thickness information its real-time application can be utilized in kinetic studies, marker experiments and studies on the redistribution of impurities during the solid-phase reaction [2–6]. This does not only drastically decrease the workload: kinetic parameters can, for example, be obtained from a single ramped annealing; it also limits the risk of overlooking important transitions in the formation process and virtually eliminates the influence of small differences in annealing procedures and specimen preparation. However, the time-consuming analysis of the vast amount of spectra produced by a single real-time RBS measurement (typically a few hundred spectra per measurement) has up to now obstructed a wide breakthrough of this powerful technique.

Conventionally, RBS spectra are analyzed using one of the standard ion beam analysis codes [7], in which computational optimization algorithms are often utilized to refine the extracted information of interest. In this process of analyzing, simulated RBS spectra are recursively compared with the data and adjusted until a convincing match is obtained. Although the consecutive spectra acquired in a real-time measurement usually show only little difference and can be analyzed using the parameters of the preceding analyzed spectrum as starting values, analyzing a full real-time RBS data set remains a huge task. Especially when real-time RBS is applied in systematic studies examining a matrix of samples having slightly different properties or examining the response to several thermal treatments, even larger data sets (1000 and more spectra) are acquired and months of analyzing are required to extract the valuable data.

* Corresponding author. Tel.: +32 16 327227; fax: +32 16 327985.
E-mail address: Jelle.Demeulemeester@fys.kuleuven.be (J. Demeulemeester).
[1] Present address: RQMP, Département de Physique, Université de Montréal, Montréal, QC, Canada H3C 3J7.

0168-583X/$ - see front matter © 2010 Elsevier B.V. All rights reserved.
doi:10.1016/j.nimb.2010.02.127

Because of the recent success booked in the automated analysis of single RBS measurements by artificial neural networks (ANNs) [8], we investigated the possibility to extend this technique to the analysis of large real-time RBS data sets. The major advantage of ANNs is that, after the time-consuming initial steps necessary to create a working network, analysis is fully automatic and practically instantaneous, virtually independent of the number of spectra fed for processing. The ANN analyzing capabilities were tested on real-time RBS data probing the solid-phase reaction of a thin Ni film with a Si substrate, and compared with the outcome of conventional analysis on the same data set. The selected system has important applications in CMOS technology, and its solid-phase reaction is therefore well documented in literature [9]. The phase sequence is well understood, and the first two phases (i.e. Ni_2Si and NiSi respectively) are characterized by a diffusion-controlled growth. Although we have already successfully applied ANN analysis to ternary systems exhibiting a much more complex growth [3] and to metal germanide growth where the overlapping metal and germanide RBS signals complicate the analysis [10], we use this rather simple physics case as an example. Hence, all attention can be drawn to the use of ANNs to analyze real-time RBS data sets, rather than to explaining the complex diffusion behavior.

2. Artificial neural networks

Artificial neural networks are program codes based on neuron-like building blocks designed to emulate data processing in the human brain [11]. ANNs are trained to solve specific problems by learning to relate numerous possible inputs to the corresponding output parameters without requiring the implementation of the physics determining this problem. Because of their intelligent design ANNs are well suited for processing incomplete data sets and noisy signals prone to statistics, which makes them applicable in the field of automated pattern recognition (where conventional software tends to fail), e.g. medical diagnosis, handwriting recognition, speech recognition, etc. Artificial neural networks have already been implemented successfully for several experimental techniques, including ion beam analysis techniques [8,12], infrared spectroscopy [13], Mössbauer spectroscopy [14,15] and analysis of synchrotron nuclear resonant scattering data [16].

An artificial neural network consists of an input and output node array connected through several node layers in between, as schematically represented in Fig. 1. These nodes are mutually connected with all nodes of the neighboring layer(s) and propagate information with a weight specific for each connection. The output of a single node is a function (usually a sigmoid) of the summed and weighted inputs from the previous node layer. These weights

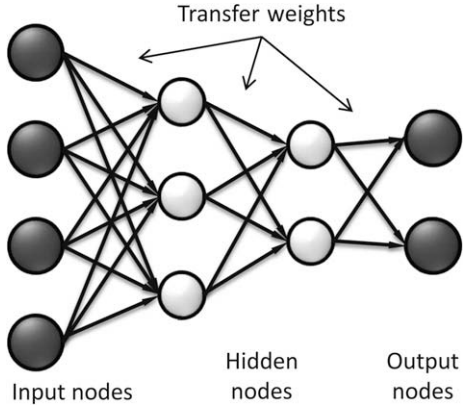

Fig. 1. A schematic representation of an artificial neural network consisting of two hidden node layers interconnecting the input and output layer via transfer weights.

are intended to model the synaptic efficiencies in the human brain. It is assumed in general, that the learning process in human brains is realized by adapting the efficiencies with which information is passed between the neurons. Similarly, an ANN can be trained to solve a specific set of problems by adjusting all the weights of the connections between the nodes. For ANNs performing the analysis of ion beam analysis (IBA) data, the input to the network consists of the essential part of the IBA spectrum. The relevant physical parameters of interest such as thickness of constituting layers, the relative elemental concentrations, the roughness, etc. could be the output parameters of the network. Consequently this implies that for each fundamentally new problem, e.g. analyzing RBS data on a totally new type of system, a new network, able to operate within the specific boundaries defining the problem, needs to be trained.

One of the standard methods to train an ANN is called *supervised learning* [11]. Supervised learning basically means that a *training set* containing numerous examples with well-known corresponding output parameters is fed to the network repeatedly to calculate the network output using a specific set of weights. After each iteration a network error is calculated according to the following equation (for simplicity only a single output node is considered):

$$E = \frac{1}{2}\sum_{n}^{N}(y_n - o_n)^2, \tag{1}$$

with N the number of examples in the training set, y_n the output calculated by the network, and o_n the desired correct output. In turn all weights are adjusted by the backpropagation algorithm [11] to minimize the network error E, i.e. training the network. As a figure of merit and a criterion to stop the training process one uses the mean-square error (MSE), given by

$$\varepsilon_{\mathrm{MSE}} = \sum_{i}\frac{(y_i - o_i)^2}{(o_i - \bar{o})^2}, \tag{2}$$

summed over the full set, with $\bar{o}$ the mean value of that specific output parameter. After each training iteration, the MSE is calculated on a similar but independent test set containing unseen spectra. This is necessary to avoid the well known problem of *overtraining*, in which the ANN learns to analyze the training set by heart. In practice, overtraining means that the ANN loses its generalizing capabilities, and cannot handle the analysis of new unknown data. Overtraining can be recognized easily from an increase in MSE on the test set while the MSE on the training set keeps on improving. Hence, once a minimal MSE is reached on both training set and test set, the training of the network is optimal and the ANN can be applied to the experimental data set, containing unseen data as well.

One of the most important criteria to obtain a well-functioning network is the quality of the training set. It is indispensable to have a realistic training set in the sense that the sampling space should at least cover all experimental possibilities. Artificial neural networks are only capable of interpolation in sampling space, they are unreliable when extrapolating. A training set may consist of experimental data as well as simulated data. Whenever a good computational model is available, it is far more beneficial to chose for the latter option. This approach offers a perfect control over the sampling space and allows to keep the training set as general as possible. The upper and lower limits as well as the distribution in between can be controlled, and in general a large training set can be obtained in a relatively short time window. A training set can for instance be generated by a code that repeatedly generates the experimental and sample parameters and prompts a conventional simulation program to calculate the corresponding spectrum. All simulated spectra should be convoluted with Poisson noise to imitate experimentally acquired data. The time needed for the construction of the training set and the training of the

network merely depends on the speed of the simulation program and the available computing power. Once the network is trained, hundreds of experimental spectra (a typical number for one real-time RBS measurement) can be analyzed instantaneously.

3. Real-time RBS

In real-time RBS, backscattering data are collected during the thermal treatment of the sample. For this purpose a heating filament and temperature controller are connected to the sample holder, on which the sample is mounted with conducting silver paste. The temperature of the readout is calibrated using the eutectics of Au–Si and Al–Si at 363 °C and 577 °C, respectively. A cold trap allows to maintain a vacuum better than $\sim 10^{-7}$ mbar during the thermal treatment. To avoid black body radiation to interfere with the backscattering collection at elevated sample temperatures, a ruggedized detector is used, stopping photons without adding too much straggling to the backscattered particles. Sufficiently high incident beam currents (50–70 nA) are maintained to allow fast data acquisition and therefore a relevant time and temperature resolution on the thermal process, without creating too much pile-up obstructing a straightforward data analysis. Every 30 s an RBS spectrum is collected. For the analysis, multiple spectra (typically 4) are assembled into a single spectrum in order to obtain good statistics (6–8 μC). In this way analyzable RBS spectra are produced, covering the thermal treatment with a time resolution of 2 min. Real-time RBS data are conveniently plotted in a contour plot such as in Fig. 2. The contour plot is constructed from the consecutively acquired RBS spectra, with the time (or temperature) axis running from bottom to top. Every horizontal line in such a contour plot corresponds to an RBS spectrum, with a color scale representing the backscattering yield.

This technique has already been applied successfully to many thin film solid-phase reaction studies. In binary systems real-time RBS can easily reveal the phase sequence, and the kinetic parameters can be extracted from the thickness information. In ternary systems real-time RBS allows to study the redistribution of all elements during the reaction enabling a thorough study of the influence of the added element on the thin film growth. When applied to marker studies, the continuous probing of the marker movement allows to determine the dominant diffusing species during the growth of a specific phase.

Theron et al. particularly highlighted the strengths of this technique by showing that the kinetic parameters of a solid-phase reaction (activation energy E_a and pre-exponential factor D_0) can be extracted from a single ramped anneal [2], whereas other techniques usually require several ramped annealings (Kissinger analysis) [17] or several isothermal annealings to construct an Arrhenius plot. As such, the full kinetics can be obtained from a single measurement, which eliminates the risks arising from irreproducibilities in sample preparation and experimental conditions. To extract the kinetic parameters for a diffusion-controlled process with diffusion coefficient $D = D_0 \exp(-E_a/k_B T)$, the squared thickness of the growing phases is plotted as a function of temperature and fitted (as described in Ref. [2]) with an exponential function containing the activation energy E_a and pre-exponential factor D_0.

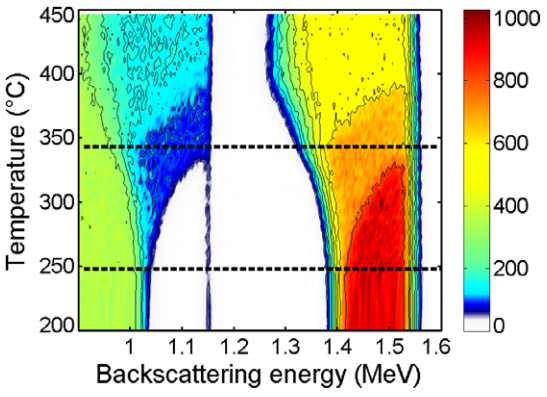

Fig. 2. Real-time RBS measurement on an 80 nm thick Ni film on Si(100) capped with 7 nm Si, ramp-annealed at 2 °C/min. The dashed lines indicate the points where the growth of a new phase is initiated.

4. Experimental details

The investigated sample consists of an 80 nm thick Ni film deposited by molecular beam epitaxy (MBE) onto a Si(100) wafer. The substrate was chemically cleaned with the standard RCA procedure and the deposition was carried out in UHV ($< 10^{-10}$ mbar). Subsequently a 7 nm thick Si capping layer was deposited in the same MBE-setup to prevent oxidation of the Ni layer. Real-time RBS measurements were performed with a 2 MeV He^+ beam, incident angle of 35° and backscattering angle of 165°. While performing the RBS experiment the sample was annealed at a constant heating rate of 2 °C/min in high vacuum ($< 10^{-7}$ Torr). Every 30 s an RBS spectrum was collected. For the analysis, 4 spectra were assembled in one spectrum resulting in a temperature resolution of 4 °C on the annealing process.

All spectra were first analyzed in a conventional way using RUMP [18]. The results were used as a reference to test the ANN's analyzing capabilities. The ANNs were trained on a training set of 18,000 spectra and a test set of 2000 spectra generated by NDF [19]. Based on previous experiences with ANN analysis we chose to use a network architecture containing only two hidden layers [8]. The training set was created such that all possible sample compositions throughout the annealing sequence are taken into account. The thickness of the present layers is chosen randomly between 0 at./cm^2 and an upper boundary depending on the phase stoichiometry and the total amount of Ni available in the sample. In order to make the ANN capable of dealing with real data, random but realistic roughness was added to the growing layers, and a small spread on beam energy and detector resolution were applied to finally convolute the full spectrum with Poisson noise. Only the thicknesses of the three phases (Ni, Ni_2Si and NiSi) were required as an output of the ANN.

5. Results

The solid-phase reaction (SPR) of a thin Ni film on a Si substrate has been studied extensively because of its importance in CMOS technology. The solid-phase reaction is characterized by the following phase sequence: [9]

$$Ni \rightarrow Ni_2Si \rightarrow NiSi \rightarrow NiSi_2.$$

First Ni transforms into a Ni_2Si film mainly via Ni diffusion into the Si substrate [20]. Once the Ni has completely transformed into Ni_2Si, NiSi starts to form at the Ni_2Si/Si interface. This diffusion-controlled growth continues until a uniform NiSi film is obtained. The formation of the $NiSi_2$ phase from NiSi is known to be nucleation-controlled and will only be initiated at elevated temperatures (800 °C). Since these temperatures are out of reach for the experimental apparatus, this latter reaction is not expected to be observed in this real-time RBS measurement.

5.1. Conventional analysis

In the real-time RBS measurement (Fig. 2) two main regions in backscattering energy can be distinguished, wherein the highest

backscattering energy strip (from approximately 1.26–1.56 MeV) represents the Ni signal and the lowest energy part (below 1.15 MeV) is produced by backscattering from Si. The narrow line visible at lower temperatures (at approximately 1.15 MeV) corresponds to the thin Si cap on top of the Ni film, and is therefore a useful guide to the eye to judge whether the Si from the substrate has reached the surface in the solid-phase reaction (i.e. whether Ni has completely transformed into a silicide). In the contour plot a transformation of one phase into the next phase is represented by a transition in color (in the Si as well as in the Ni RBS signal) and by a bending contour line (increasing thickness) separating the two regions. For each temperature the position of this contour depicts the position of the interface between the shrinking and the growing phase in the film. The curvature of these contours as a function of temperature is thus a measure for the growth rate of the growing phase. As can be deduced from the real-time RBS measurement (Fig. 2), two phase transformations occur. The starting point of the formation of each new phase is indicated by the dashed lines in Fig. 2.

At first sight the Ni silicide formation thus proceeds as one would expect. The bending of the Ni and Si contours from approximately 250 °C to approximately 340 °C signals the growth of Ni_2Si , the first phase in the thin film Ni silicide phase sequence. As Ni diffuses into the substrate, Si appears at higher backscattering energies because of the apparent movement towards the surface. Once the Si contour has reached the Si surface energy the Ni film has completely transformed into Ni_2Si (indicated by the dashed line at 340 °C in Fig. 2). From that point onwards NiSi forms as indicated by the subsequent bending in the Ni and Si contours, and continues until a homogenous NiSi film is obtained (at approximately 400 °C). The NiSi film remains stable until the end of the annealing since the $NiSi_2$ nucleation temperature (800 °C) is not reached.

Fig. 3 shows the thickness of the Ni, Ni_2Si and NiSi layers as a function of the annealing temperature (solid symbols) as obtained from the conventional analysis. The thickness is expressed in the number of Ni atoms (10^{15} Ni at./cm^2) present in a certain phase. As demonstrated in this figure the real-time RBS data allow a quantitative analysis of the silicide thin film growth. Both reactions, i.e. the formation of Ni_2Si and the formation of NiSi, can be distinguished and contain enough data points for each of the phases to characterize the phase growth. Although most of the spectra can be analyzed quite fast, taking the parameters of the previous spectrum as an initial guess for the local search routine in RUMP (PERT) [21], it easily requires several days to fully analyze the real-time RBS measurement.

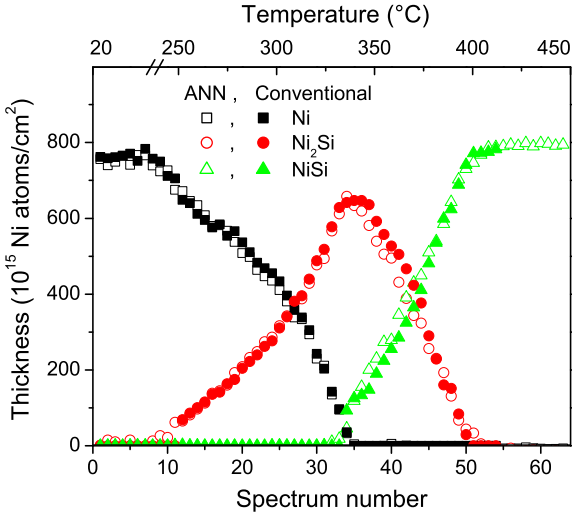

Fig. 3. Overview of the thickness evolution of Ni (squares), Ni_2Si (circles) and NiSi (triangles) during a 2 °C/min ramped annealing of an 80 nm thick Ni film capped with 7 nm Si on Si(100). The results are obtained by conventional analysis (solid symbols) and by ANN analysis (open symbols).

5.2. ANN analysis

For the specific system investigated we used a network consisting of 161 input nodes and 3 output nodes (i.e. the thickness of the three phases) connected through two hidden layers containing 50 and 20 nodes respectively, i.e. (161, 50, 20, and 3). Only 161 relevant channels, covering backscattering energies from 0.8 to 1.6 MeV, were selected to constitute the data input. The lowest channels containing only information on the Si substrate, and the channels above the Ni signal were barred from the input. As mentioned before, the training set (18,000 examples) and the test set (2000 examples) were generated by a code that automatically prompts NDF to calculate the RBS spectrum corresponding to the given parameters. The thickness of the composing layers (i.e. capping, Ni, Ni_2Si , and NiSi layer) was varied between realistic values, and a random but relevant distribution of other contributing parameters, e.g. collected charge, detector resolution, layer roughness, straggling factor and beam energy was included in the training and test set as well. Since we were only interested in the thickness of the growing or disappearing Ni, Ni_2Si , and NiSi layer, only those three parameters were requested as an output from the network. The creation of the training and test set was accomplished within 12 h with a Pentium 4 processor running at 2.66 GHz, whereas the training of the network was realized within half an hour. Although numerous spectra (63 in total) needed to be analyzed, it required only a fraction of a second for the ANN to process the data and come up with the output that is shown in Fig. 3 (open symbols).

To evaluate the ANN performances, the network output (open symbols) is overlayed with the conventional analysis (solid symbols) in that figure. As can be seen the agreement between both analysis results is striking and covers the full real-time RBS measurement. Not only is the ANN capable of distinguishing between the three possible phases, the network is also able to determine the thickness of each of the phases with great accuracy. This is a remarkable result considering that the network is actually trained on a very general training set containing a wide variety of RBS spectra. The thickness of each of the phases was for instance (necessarily) varied between thicknesses corresponding to a Ni content of 0 and 850×10^{15} at./cm^2. Nevertheless the ANN had no problem to ascribe the correct thickness to each of the phases for each spectrum. In general it is a good idea to restrict the network output to the parameters of interest only. Having less output parameters allows one to train the network with a simpler architecture and thus less connections, which results in a decrease in computation time needed to train the network. Additionally, simpler networks usually produce more reliable results [12].

6. Discussion

The most difficult task in the analysis is to pinpoint the moment at which the growth of a new phase is initiated, as the initial stages of growth can easily be overlooked or be mistaken as an increase in roughness. In practice, when analyzing in a conventional way, one tries to overcome this problem by working backwards; i.e. analyze a spectrum where the new silicide phase has already grown to a reasonable thickness, and successively analyze preceding spectra to work towards the initial point. This basically means that the experimentalist is using his/her knowledge on the solid-phase

reaction of the studied system to assist in the analysis of the full real-time RBS measurement. In contrast to this, the network has no knowledge of the expected phase sequence and growth kinetics, and processes all spectra independently from each other. Nevertheless the ANN performs exceedingly well in identifying the initial stages of growth. Whereas in the conventional analysis at spectrum 12 and 34 (Fig. 3) a large discrete step from zero thickness to a certain finite thickness of the new silicide phase can be observed, the ANN reveals the transition more fluently without deviating from the conventional analysis. Moreover, the ANN analysis can be taken as a confirmation that the judgement of the experimentalist to include a new phase in the analysis at that certain point was a correct decision. Artificial neural networks exclude any influence of the experimentalist and provide therefore a neutral and reliable analysis.

As an additional control of the performance of the ANN one can take the output of the neural network, feed it to simulation software and compare the simulation with the data. This is for example done in Fig. 4 for spectra acquired during the real-time RBS measurement at the three stages in the reaction sequence, i.e. pure Ni (RT), growth of Ni_2Si (at 311 °C) and growth of NiSi (at 384 °C). The Ni, Ni_2Si and NiSi thicknesses were taken from the ANN output and were left unaltered for the simulation. A capping layer and realistic amount of roughness on the growing layer were added to the sample structure used to make the simulation. The convincing match for these spectra taken at the different stages of growth provides again a confirmation on the excellent qualitative analysis capabilities of the used ANN. With the available simulation software one can easily generate such simulations using the ANN output for all the spectra in the real-time measurement in an automated way. This allows to evaluate the performance of the ANN over the entire data set.

In general it can be stated that spectra with corresponding output parameters which are well-covered by the training set sampling space are expected to yield a correct ANN analysis. Spectra related to parameters far away from the sampling space average have a large probability to yield meaningless results, without a warning from the network. An alternative solution to avoid that corrupt results remain undetected is thus to check whether the individual spectra are outliers or not, prior to passing them through the network for analysis. This can be done by training an additional ANN that classifies spectra as "acceptable" or "not acceptable", based on the sampling space of the training set [22].

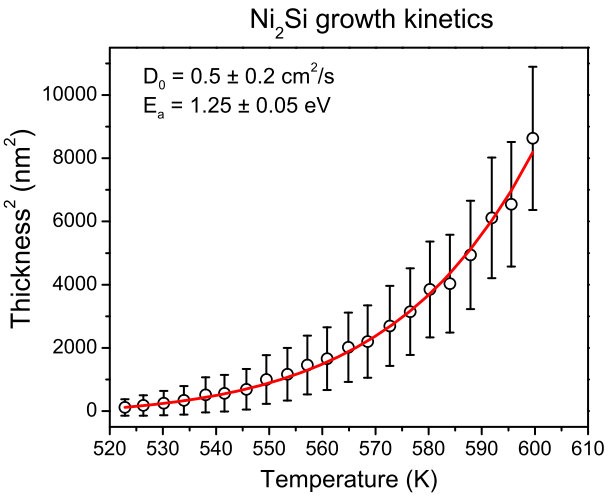

Fig. 5. Squared thickness of the growing Ni_2Si phase as a function of temperature as obtained from the ANN analysis of the real-time RBS measurement during a ramped annealing at 2 °C/min (data points). The fit (solid line) allows to extract the activation energy E_a and the pre-exponential coefficient D_0 characterizing the Ni_2Si growth kinetics.

Hence, the experimentalist is warned whenever the ANN is likely to analyze a spectrum beyond its analyzing capabilities.

As an example the growth kinetics of the Ni diffusion governing the Ni_2Si and NiSi growth were extracted from the results obtained via ANN analysis. Special efforts were made not to get trapped in local minima during the fitting procedure, which often results in a seemingly good fit, but incorrect values for the apparent activation energy and pre-exponential coefficient. Therefore the variance between the data and the fit were calculated while moving E_a and D_0 through parameter space, in order to find the absolute minimum. The Ni_2Si growth kinetics are fitted in Fig. 5 and yield an activation energy E_a of 1.25 ± 0.05 eV and a pre-exponential coefficient D_0 of 0.5 ± 0.2 cm^2/s. The NiSi growth kinetics are characterized by an activation energy E_a of 1.34 ± 0.06 eV and a pre-exponential coefficient D_0 of 2.7 ± 0.3 cm^2/s. The fit is displayed in Fig. 6. In literature different values can be found for the Ni_2Si growth kinetics ($E_a \sim 1.3$—1.6 eV) as well as for the NiSi growth

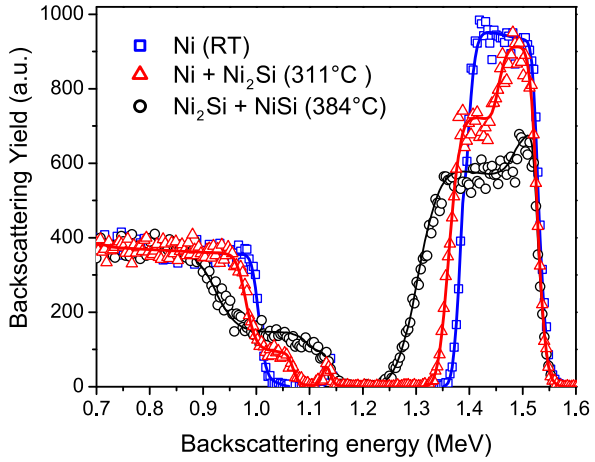

Fig. 4. Selection of RBS spectra acquired during the real-time RBS measurement of an 80 nm thin Ni film on Si(100) at several stages of the solid-phase reaction, i.e. as deposited (at RT, squares), during Ni_2Si growth (at 311 °C , triangles) and during NiSi growth (at 384 °C , circles). The simulations based on the ANN output are represented by the solid lines.

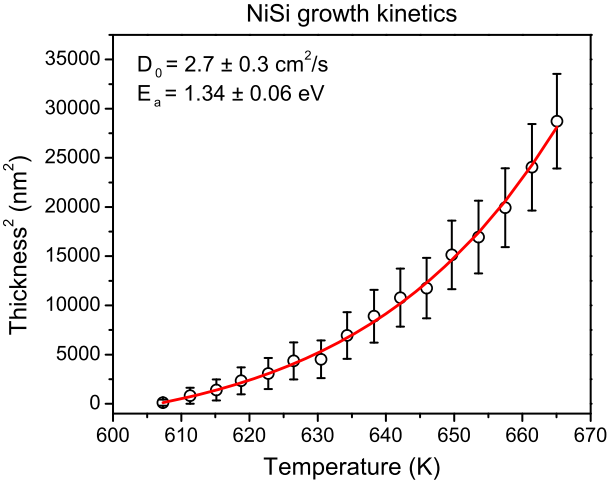

Fig. 6. Squared thickness of the growing NiSi phase as a function of temperature as obtained from the ANN analysis of the real-time RBS measurement during a ramped annealing at 2 °C/min (data points). The fit (solid line) allows to extract the activation energy E_a and the pre-exponential coefficient D_0 characterizing the NiSi growth kinetics.

kinetics ($E_a \sim 1.2$—1.8 eV) [23]. These discrepancies can be related to several causes as different impurity concentration in the thin film related to the deposition method, influences of the capping layer, use of a different technique to extract the kinetic parameters, etc. In this case the obtained kinetic parameters compare best to the results obtained from RBS data acquired from isothermal annealings for the growth of Ni_2Si ($E_a = 1.35 \pm 0.1$ eV and $D_0 = 0.745\ cm^2/s$) [24], as well as for the growth of NiSi ($E_a = 1.55 \pm 0.1$ eV) [25].

7. Conclusions

We have constructed, trained and applied an artificial neural network (ANN) to analyze RBS data of the growth of Ni silicide thin films. The ANN is clearly capable of extracting the thickness of the composing layers in the reacting system with the same quality as conventional analysis. The remarkable difference, however, is the time scale involved. Whereas conventional analysis of huge real-time RBS data sets is extremely time-consuming and hence discouraging, it takes the ANN only a fraction of a second to extract the parameters of interest from the numerous RBS spectra. Although it takes a few days to create a proper and optimal training set and train the ANN, the benefits still hold. Especially when ANNs are applied in systematic real-time RBS studies where similar samples are annealed at several thermal treatments, the use of the fast analysis capabilities of ANNs become virtually indispensable. The combination of real-time RBS and ANN analysis is thus extremely useful and efficient in dedicated studies requiring a matrix of samples, e.g. examining the solid-phase reaction in ternary systems containing varying concentrations of an impurity, marker studies, kinetic studies, etc. Once the ANN is trained it does not matter how many spectra have to be analyzed. Furthermore, ANNs exclude the influence of the experimentalist on the results and produce a reliable neutral analysis.

Acknowledgements

This work was supported by the Fund for Scientific Research, Flanders (FWO), the Concerted Action Program (GOA/2009/006) and the CREA program (CREA/07/005) of the KULeuven, the Inter-university Attraction Pole (IAP P6/42), the Center of Excellence Programme (INPAC EF/05/005) and the Bilateral Cooperation between Flanders and South Africa (BIL 04/47). The authors also wish to thank the Material Research Group at iThemba LABS for the use of their facilities.

References

[1] C.C. Theron, J.A. Mars, C.L. Churms, J. Farmer, R. Pretorious, Nucl. Instrum. Methods B 139 (1998) 213.
[2] C.C. Theron, J.C. Lombard, R. Pretorious, Nucl. Instrum. Methods B 161 (2000) 48.
[3] J. Demeulemeester, D. Smeets, C. Van Bockstael, C. Detavernier, C.M. Comrie, N.P. Barradas, A. Vieira, A. Vantomme, Appl. Phys. Lett. 93 (2008) 261912.
[4] D. Smeets, J. Demeulemeester, K. De Keyser, D. Deduytsche, C. Detavernier, C.M. Comrie, C.C. Theron, C. Lavoie, A. Vantomme, J. Appl. Phys. 104 (2008) 093533.
[5] D. Smeets, J. Demeulemeester, D. Deduytsche, C. Detavernier, C.M. Comrie, C.C. Theron, C. Lavoie, A. Vantomme, J. Appl. Phys. 104 (2008) 1035838.
[6] G. Berning, C.C. Theron, H.C. Swart, Appl. Surf. Sci. 157 (2000) 129.
[7] N.P. Barradas, K. Arstila, G. Battistig, M. Bianconi, N. Dytlewski, C. Jeynes, E. Kótai, G. Lulli, M. Mayer, E. Rauhala, et al., Nucl. Instrum. Methods B 262 (2007) 281.
[8] N.P. Barradas, A. Vieira, Phys. Rev. E 62 (2000) 5818.
[9] J.P. Gambino, E.G. Colgan, Mater. Chem. Phys. 52 (1998) 99.
[10] W. Knaepen, D. Smeets, J.L. Jordan-Sweet, A. Vantomme, C. Detavernier, C. Lavoie, Unpublished results.
[11] C.M. Bishop, Neural Networks for Pattern Recognition, Oxford University Press, Oxford, 1995.
[12] H.F.R. Pinho, A. Vieira, N.R. Nené, N.P. Barradas, Nucl. Instrum. Methods B 228 (2005) 383.
[13] L. Duponchel, C. Ruckebusch, J.P. Huvenne, P. Legrand, J. Near Infrared Spectrosc. 7 (1999) 155.
[14] H. Paulsen, R. Linder, F. Wagner, H. Winkler, S.J. Pöppl, A.X. Trautwein, Hyperfine Interact. 126 (2000) 421.
[15] P.A.D. Souza, V.K. Garg, G. Klingelhofer, R. Gellert, P. Gutlich, Hyperfine Interact. 139–140 (2002) 705.
[16] N. Plankaert, J. Demeulemeester, B. Laenens, D. Smeets, J. Meersschout, C. L'abbé, K. Temst, A. Vantomme, J. Synchrotron Rad. 17 (2010) 86.
[17] H.E. Kissinger, Anal. Chem. 29 (1957) 1702.
[18] L.R. Doolittle, Nucl. Instrum. Methods B 9 (1985) 344.
[19] N.P. Barradas, C. Jeynes, R.P. Webb, Appl. Phys. Lett. 71 (1997) 291.
[20] W.K. Chu, H. Kraütle, J.W. Mayer, H. Müller, M.-A. Nicolet, K.N. Tu, Appl. Phys. Lett. 25 (1974) 454.
[21] L.R. Doolittle, Nucl. Instrum. Methods B 15 (1986) 227.
[22] N.P. Barradas, A. Vieira, R. Patrício, Phys. Rev. E 65 (2002) 066703.
[23] K. Maex, M. Van Rossum, Properties of Metal Silicides, INSPEC, The Institution of Electrical Engineers, London, United Kingdom, 1995, ISBN: 0 85296 859 0.
[24] P.M. Jardim, W. Acchar, W. Losch, Appl. Surf. Sci. 137 (1999) 163.
[25] C.-D. Lien, M.-A. Nicolet, S.S. Lau, Thin Solid Films 143 (1986) 63.